Available online at www.sciencedirect.com
SCIENCE DIRECT®
Food Chemistry 92 (2005) 45–54
Food Chemistry
www.elsevier.com/locate/foodchem

Testing of microencapsulated flavours by electronic nose and SPME–GC

Renata Baranauskienė [a], Petras Rimantas Venskutonis [a,*], Algirdas Galdikas [b], Daiva Senulienė [b], Arūnas Šetkus [b]

[a] Department of Food Technology, Kaunas University of Technology, Radvilėnų pl. 19, Kaunas LT-50015, Lithuania
[b] Semiconductor Physics Institute, A. Goštauto 11, Vilnius LT-01108, Lithuania

Received 23 January 2004; received in revised form 7 May 2004; accepted 24 June 2004

Abstract

The present study deals with the use of metal oxide gas sensors and the headspace techniques for microencapsulated essential oils of thyme, oregano and cassia. The volatile compounds released from the microencapsulated flavours were tested by an array of the gas sensors. The features of individual odours were described using an analysis of the transient responses of the sensors to the aroma. The coating materials were graded with respect to the leakage of volatile components. The volatile compounds leaking from the microencapsulated flavours were collected by the headspace SPME technique and analysed by GC–MS. Based on the results, the Hi Cap 100 was considered to be the least emitting coating material while the Encapsul 855 was the most leaking matrix in our study.

Keywords: Microencapsulation; Thyme; Oregano; Cassia; Essential oil; Electronic nose; Gas sensors; Headspace; SPME; GC; GC–MS

1. Introduction

Qualitative and quantitative assessment of volatile aroma components released from flavourings is very important in the quality control used by the aroma and food industries. Instrumental analysis (GC, GC–MS, HPLC, SPME) and evaluation by sensory panel are the two classical approaches to the problem of the quality, however most of them are expensive, time consuming and do not provide an immediate result. Electronic olfaction systems, so-called "electronic noses" (e-noses), were recognised to be promising techniques in the development of rapid tests in food control (Ampuero & Bosset, 2003). This method was successfully employed for detection of various odours including simple gases and complex mixtures during the last decade (Ampuero & Bosset, 2003). The success in evaluation of the foodstuff quality and freshness was related with the main advantages of the nose, namely high sensitivity, short analysis time and high accuracy of the identification (Brezmes et al., 2001; Di Natale et al., 2001; Guadarrama, Fernandez, Iniguez, Souto, & de Saja, 2001; Maekawa, Suzuki, Takada, Kobayashi, & Egashira, 2001; Penza, Cassano, Tortorella, & Zaccaria, 2001). In spite of various advantages, it was commonly recognised that the e-nose cannot be used instead of the analytical methods (e.g. GC–MS) that generate a huge data set containing complete information about the smell composition. On the other hand, the e-nose is preferable for development of an automatic/on-line evaluation system acceptable in monotonous routine of practical applications.

* Corresponding author. Tel.: +370 37 456426; fax.: +370 37 456647.
E-mail address: rimas.venskutonis@ktu.lt (P.R. Venskutonis).

0308-8146/$ - see front matter © 2004 Elsevier Ltd. All rights reserved.
doi:10.1016/j.foodchem.2004.06.048

In general stationary signals are usually collected from a number of electronic nose sensors exposed to an odour. The odours are recognised by special programs based on signal analysis of an array of the sensors (Brezmes et al., 2001; Di Natale et al., 2001; Guadarrama et al., 2001; Maekawa et al., 2001; Penza et al., 2001). It was proved recently that processing of dynamic responses of the sensors is much more efficient for the recognition of smell features than standard approach (Galdikas, Mironas, Senulienė, & Šetkus, 2000; Katoa et al., 2000; Nakata, Takemura, & Neya, 2001; Simona, Barsan, Bauera, & Weimar, 2001). In dynamic regime, time dependence of the signals is detected for the sensors switched from one working temperature to another (Katoa et al., 2000; Nakata et al., 2001; Simona et al., 2001) or exposed to a steep change in gas composition of the atmosphere (Galdikas et al., 2000). An increase in number of the parameters that characterise a target smell is the advantage of the dynamic regime if compared to the standard electronic nose with a similar number of the sensors.

In the present study, transient response electronic nose was applied for the evaluation of microencapsulated flavours. The volatile components released from microencapsulated thyme, oregano and cassia essential oils, respectively, were analysed with an array of solid-state gas sensors. The composition of essential oils was analysed by capillary GC, GC–MS and static headspace methods. The flavour profile in headspace of microencapsulated aromas was analysed by SPME. The results of the gas sensors were compared with that from the SPME–GC. The data obtained can be useful in further developments of rapid methods in food flavour control.

2. Materials and methods

2.1. Materials

Cassia (*Cinnamomum cassia*), thyme (*Thymus vulgaris*) and oregano (*Origanum vulgare*) essential oils (EO) were selected as core materials, all from Frey&Lau GmbH, (Henstedt-Ulzburg, Germany). Commercial modified food starches named Hi Cap 100 (derived from waxy maize), Capsul E (derived from tapioca), Encapsul 855 (tapioca dextrin, corn dextrin) and N LOK (food starch modified with corn syrup added) obtained from the National Starch&Chemical (Hamburg, Germany) were used as encapsulating agents.

2.2. Preparation of microencapsulated flavours

The solutions of coating matrixes, 30% concentration (w/w), were prepared by reconstituting and dispersing of dried powders in 40 °C deionised water, and after cooling they were mixed overnight to enhance hydration. EO (15% w/w of matrix solids) was emulsified into the hydrated coating material. Homogenisation was accomplished by using Ultra Turrax Ika 25 basic homogenizer (Janke&Kunkel GmbH & Co., Germany) operating at 20500 rpm for 5 min. Emulsions were spray-dried in a Büchi 190 mini spray dryer (Donau, Switzerland) under the following parameters: spray nozzle (inlet) temperature 180 ± 5 °C, outlet air temperature 90 ± 5 °C, pressure 750–800 mm/H_2O (Bylaitė, Venskutonis, & Maždžierienė, 2001). Dried products were packed into the glass containers and stored in laboratory freezer until further investigation.

2.3. Solid phase-microextraction and static headspace analysis

Solid phase-microextraction (SPME) was performed with three different fibres, namely polydimethylsiloxane (PDMS, 100 μm), carbowax-divinylbenzene (CW-DVB, 65 μm) and polyacrylate (PA, 85 μm), all from Supelco (Bellefonte, PA). For headspace SPME sampling, 0.1 g of encapsulated flavours were placed in a 4 mL vial, closed with an open hole cap faced with a PTFE/white silicone septum and equilibrated in a Gerber Liebisch-Bielefeld 14 thermostat (Gerber Instruments, Effretikon, Germany) at 40 °C for 30 min. The fibre was exposed to the headspace of encapsulated flavours during 5 min at 40 °C. Afterwards, the fibre was withdrawn into the housing, the SPME device was removed from the sample vial and the fibre was desorbed into the GC–MS injector.

For the conventional static headspace 100 μL of each oil was placed into 20 mL headspace vial that was sealed hermetically with a PTFE/butyl-coated septum and silver aluminium cap. The Hewlett–Packard HP 7694E headspace sampler was used to monitor the static headspace of oil volatiles. Samples were equilibrated for 20 min at 40 °C. The headspace loop (1 mL headspace sampling) and transfer line temperature was set at 60 and 80 °C respectively and desorbed volatiles were analysed on GC–MS.

2.4. Gas chromatography–mass spectrometry

Gas chromatography–mass spectrometry (GC–MS) analyses were performed using a HP 5890 (II) gas chromatograph coupled to an HP 5971 series mass selective detector (Hewlett–Packard, Avondale, PA) in the electron impact ionization mode at 70 eV, the mass range was *m/z* 30–550. Volatile compounds were separated using an HP-5 MS capillary column (polydimethylsiloxane, 5% diphenyl, 30 m length, 0.25 mm i.d., 0.25 μm film thickness, Hewlett–Packard). The temperature was programmed from 40 °C (2 min) to 180 °C at 4 °C min^{-1} and finally increased to 270 °C at 10 °C min^{-1} (5 min hold). Helium was used as a carrier gas at a linear flow

velocity of 36.2 cm s^{-1} at 40 °C or 1.0 mL min^{-1} volumetric flow.

For the analyses of the headspace of the essential oil split mode was used at a ratio of 1:5 and an injector temperature of 250 °C. Thermal desorption of volatile analytes adsorbed on the SPME fibres was carried out in the GC injector port at 250 °C for 3 min in a splitless mode.

The components were identified by comparison of their Kováts retention indices (KI) relative to C_8–$C_{30,32}$ *n*-alkanes (Sigma Chemical Co., St. Louis, MO), obtained on HP-5 MS column with those provided in literature (Adams, 2001) and by comparison of their mass spectra with the data provided by the NIST, NBS 75K/Wiley and EPA/NIH mass spectral libraries. Positive identification was assumed when a good match of mass spectrum and KI was achieved. The content of the individual constituents was expressed in arbitrary units (au), the total ion current of the relevant peaks detected by GC–MS.

2.5. Analysis with an array of solid-state gas sensors

To our knowledge, this method was not yet employed for the analysis of the encapsulated EO. In our method, metal oxide gas sensors were temporary exposed to the volatile compounds blown from the powder of the encapsulated EO. If the aroma was injected in the atmosphere the resistance of the sensors changed and the response signals were detected. The array of the electronic nose was composed of four gas sensors. The sensors SO18-23, SO18-24 and ITO 16 were home made (Semiconductor Physics Institute, Lithuania) and based on tin and indium oxides thin films, while TGS800 was tin oxide ceramic sensor from FIGARO. The sensors were non-selective to gases but the response of individual sensor to the same gases (e.g. CO, H_2,C_2H_5OH, NO_x) was different at the same conditions of the experiment.

The array was exposed to a steep change in the composition of the atmosphere. For this, a two-flow-channels system was employed. In this system, a stream of clean synthetic air was flowing in one of the channels. In other channel, a mixture of the synthetic air and the volatile constituents released from the encapsulated oils was flowing. In the channels, the flow rates of the streams were similar. Humidity of the air was also similar in both channels. Relative humidity was fixed by the computerised system at about 50% and maintained constant during the tests. Switching between the two flows had produced a steep change in gas composition in the test chamber with the sensors. Details of the equipment are described elsewhere (Galdikas, Kancleris, Senulienė, & Šetkus, 2003).

Time dependencies of the response signals were measured for each sensor in the array. The sampling rate of the signal was 1 point per second for each sensor.

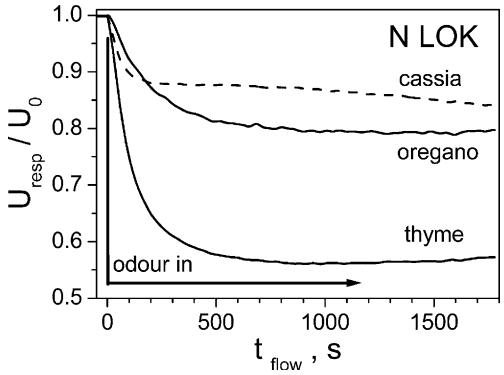

Fig. 1. Transients of the relative response signals of the SO18-23 sensor to odours released from the EO encapsulated in the N LOK matrix (the relative signal U_{resp}/U_0 represent the ratio between the sensor signal U_{resp} in the atmosphere with the smell and the signal U_0 in the clean air, t_{flow} is the measurement time).

Typical responses to the smell of the flavours are illustrated for one of the sensors in Fig. 1. Long lasting changes were detected in some transients (e.g. cassia in Fig. 1) while the essential magnitude of the response was detected after a short period (about 1–3 min). Since the long lasting changes were expected for heavy volatile compounds, very long duration of the individual test was performed for characterisation of these compounds. On the other hand, the duration was limited by a poisoning of the gas system by the volatile compounds after the long flow in the channels. It was experimentally found that a 30 min run was optimal for these tests because the clean air signal was recovered for the sensors within about 15–20 min after restoring the clean air in the chamber. The signals of the transient responses were characterised by individual sets of pairs of the parameters. Each pair was consisting of time constant τ_i and corresponding weight coefficient a_i. According to the method, the parameters were plotted for each exposure in a graph describing a dependence of weight coefficient a_i versus time constant τ_i. Consequently, 2Dτ-images were composed for tested objects emitting volatile compounds into atmosphere. A detailed description of the method was presented in a recent report (Galdikas et al., 2003; Galdikas et al., 2000).

3. Results and discussion

3.1. Microencapsulation efficiency

Effectiveness of microencapsulation is the most important characteristic feature of the process. It mainly depends on the total oil retained in the matrixes after spray-drying and the content of the oil which was directly entrapped into the capsules. It was determined that most of the matrixes used were effective microencapsulating

agents. An exception was maltodextrin Encapsul 855, which retained the lowest amount of oils, from 51.6% (cassia) to 64.6% (oregano). Other carbohydrate matrixes retained from 79.6% (N LOK, cassia EO) to 95.1% (Capsul E, oregano EO) (Venskutonis, Boceviciute, & Plaušinaitis, 2001). The content of surface oil after spray-drying did not exceed 3–5% from the total oil retained (Baranauskienė, Venskutonis, Dewettinck, & Verhé, 2003; Bylaitė et al., 2001; Venskutonis et al., 2001).

3.2. Flavour release from encapsulated oils

SPME–GC was used to compare the release of the main compounds in the headspace of encapsulated oils. Volatile sample constituents are adsorbed on a thin, fused silica fibre, coated with a layer of an organic polymer placed in the headspace above the sample, and subsequently thermally desorbed inside a GC injection port. The SPME coatings can be classified by polarity, extraction type (absorbent or adsorbent), or size exclusivity (Shirey, 2000a). Three different SPME-coated fibres, PDMS (non-polar absorbent-type), combined CW-DVB (polar, adsorbent-type) and PA (polar, absorbent-type), were used in our study. The PDMS is a nonpolar coating, that has been known to work effectively on a wide range of analytes, both polar and nonpolar (Steffen & Pawliszyn, 1996); the PA coating is a polar phase, which readily extracts more polar analytes (Steffen & Pawliszyn, 1996). The CW-DVB-coating fibre is more polar; the affinity it has for small amines is poor, however, this fibre extracts acetic acid, aniline and other nitrogen-based aromatics efficiently (Shirey, 1999; Shirey, 2000b).

The volatile profile of thyme consists mainly of aliphatic and oxygenated terpenes. *p*-Cymene (26.3%), 1,8-cineole (16.0%), thymol (27.9%), carvacrol (6.0%) and α-pinene (5.6%) have been determined to be major quantitative constituents (Venskutonis et al., 2001). Thymol constituted >27% in the total oil and this phenolic compound is known as the most important flavouring and antimicrobial agent in thyme EO (Hulin, Mathot, Mafart, & Duffose, 1998; Marino, Bersani, & Comi, 1999; Rasooli & Abyaneh, 2004). Fig. 2 illustrates the concentration of the main compounds extracted from encapsulated thyme EO headspace by different fibres used. The concentrations of the main compounds extracted from encapsulated flavours headspace by different fibres were expressed in au related to the peak area, which provide comprehensive information about extraction efficiency as long as they are directly related to the absolute amount of a particular compound absorbed by the matrix. Such data could be closely related to the sensory properties of encapsulated flavours.

Hi Cap 100 was the most effective to retain thyme volatile oil (90.1%) and it was considered as the least leaking matrix. Total volatiles absorbed with PDMS-coating fibre from encapsulated into Hi Cap 100 thyme EO headspace was $(25.3 \pm 1.9) \times 10^6$ au. The highest enrichment to extract thyme volatile compounds was obtained with PA-coated fibre [$(669.4 \pm 71.8) \times 10^6$ au] and it is mostly related to phenolic compounds in thyme EO; the combined CW-DVB coating extracted approximately 1.9 times lower amounts of aroma constituents [$(356.9 \pm 29.8) \times 10^6$ au]. The most leaking matrix was Encapsul 855, with the biggest content of released thyme volatiles, $(13249.1 \pm 1754.6) \times 10^6$, $(1322.8 \pm 148.2) \times 10^6$ and $(2805.1 \pm 453.2) \times 10^6$ au on PDMS-, CW-DVB- and PA-coated fibres, respectively. A very high amount of *p*-cymene [$(6731.1 \pm 976.7) \times 10^6$ au] was detected in headspace of thyme encapsulated into Encapsul 855 with PDMS; while above Hi Cap 100 it constituted only $(0.5 \pm 0.03) \times 10^6$ au (Fig. 2). The same component extracted with PDMS in headspace of thyme oil encapsulated into Capsul E and N LOK constituted $(606.9 \pm 68.4) \times 10^6$ and $(370.1 \pm 49.0) \times 10^6$ au, respectively.

The volatile profile of oregano EO is quite similar to that of thyme. *p*-Cymene (30.3%), 1,8-cineole (15.4%), thymol (6.7%) and carvacrol (26.8%) have been determined to be major quantitative constituents (Venskutonis et al., 2001). The phenolic component carvacrol is the most important flavouring and antimicrobial agent in oregano EO (Hulin et al., 1998; Ultee & Smid, 2001; Velluti et al., 2003). The concentrations of the main components extracted from encapsulated oregano oil headspace by different SPME fibres are depicted in Fig. 3. Again, Hi Cap 100 matrix has shown the least leakage and amounts of volatiles extracted with PDMS, CW-DVB and PA coatings were $(132.9 \pm 5.9) \times 10^6$, $(812.8 \pm 58.8) \times 10^6$ and $(1528.0 \pm 205.5) \times 10^6$ au, respectively. Thymol and carvacrol are polar compounds and were better extracted on PA-coated fibre, $(327.0 \pm 41.6) \times 10^6$ and $(976.1 \pm 139.9) \times 10^6$ au, respectively (oregano EO into Hi Cap 100, Fig. 3). Capsul E was also capable to retain volatiles, however the flavour profile was different to that extracted from Hi Cap 100 headspace. The highest amount of volatiles was extracted with PDMS-coated fibre [$(1698.5 \pm 174.0) \times 10^6$ au]; the CW-DVB and PA coatings extracted approximately 4.8 [$(356.1 \pm 34.4) \times 10^6$ au] and 2.1 [$(810.3 \pm 99.4) \times 10^6$ au] lower amounts of aroma constituents, respectively. The most leaky matrix was Encapsul 855; the amounts of volatiles extracted with PDMS-, CW-DVB- and PA-coating fibres were $(7871.2 \pm 833.3) \times 10^6$, $(1235.2 \pm 127.1) \times 10^6$ and $(3064.7 \pm 157.1) \times 10^6$ au, respectively. Again a high amount of the monoterpene hydrocarbon *p*-cymene was detected above encapsulated oregano EO with nonpolar PDMS coating and constituted $(2883.6 \pm 317.1) \times 10^6$ au (oregano EO into Encapsul 855, Fig. 3). The monoterpene hydrocarbons are more volatile components than oxygenated ones. For instance,

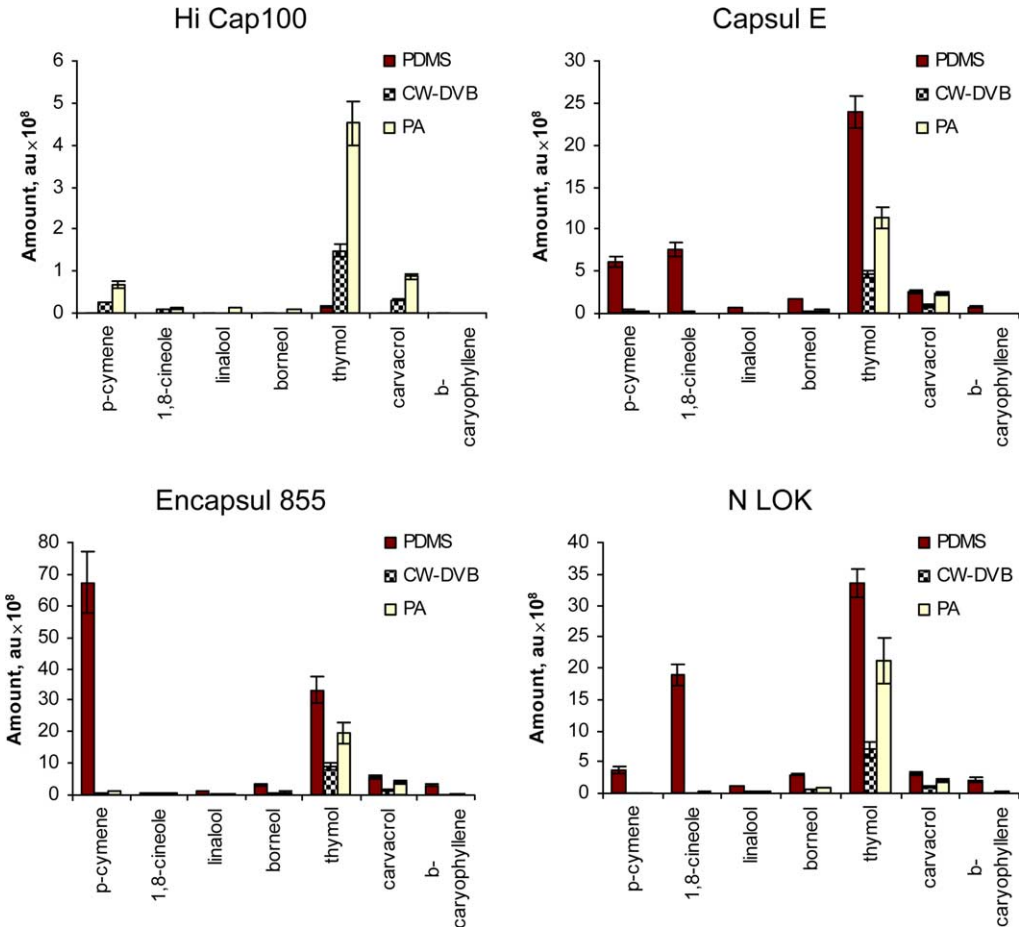

Fig. 2. Flavour profile of the main constituents in the headspace of encapsulated thyme EO, using four different encapsulating matrixes, namely Hi Cap 100, Capsul E, Encapsul 855, N LOK. Determination of the amounts of constituents was performed using SPME–GC–MS, with three different SPME fibers, namely PDMS, CW-DVB and PA.

vapour pressure of nonpolar *p*-cymene is 200 Pa at 20 °C (boiling temperature = 177 °C), while that of polar compound linalool (boiling point 198–200 °C) is almost 10 times lower (21 Pa at 25 °C); thymol (boiling point 233 °C) has even lower vapour pressure of 5.33 Pa at 20 °C (Lide, 2004). Also, Encapsul 855 showed the lowest capacity to retain oil and the highest content of surface (nonentrapped into capsules) oil.

The volatile profile of cassia EO was different from that of thyme and oregano oils. The dominant components are oxygenated monoterpenes with (*E*)-cinnamaldehyde constituting 82.2% of the total oil. It is known as the main flavouring and antimicrobial agent in cassia EO (Baratta et al., 1998; Nielsen & Rios, 2000; Velluti, Sanchis, Ramos, Egido, & Marín, 2003). The other important components were cinnamyl acetate (6.3%), *p*-methoxy-cinnamaldehyde (4.8%) (Venskutonis et al., 2001).

The concentrations of the main compounds extracted from encapsulated cassia EO headspace by different SPME fibres are presented in Fig. 4. The least leaking coating in case of cassia EO was N LOK; total amounts of volatiles constituted $(1517.5 \pm 148.3) \times 10^6$, $(343.0 \pm 23.3) \times 10^6$ and $(652.6 \pm 61.2) \times 10^6$ au on PDMS-, CW-DVB- and PA-coated fibres, respectively. Capsul E and Encapsul 855 were almost of the similar capacity to release cassia volatiles; flavour profiles and the amounts of individual components were similar. Hi Cap 100 was the least emitting coating material in case of cassia oil. The major flavouring agent of cassia oil (*E*)-cinnamaldehyde, as being a polar compound, was efficiently extracted with polar PA-coated fibre, however it was also determined in high amounts with nonpolar PDMS. The results also demonstrate that the peak areas of analytes extracted with the CW-DVB fibre were significantly lower than those extracted with other fibres used.

The efficiencies of the SPME fibres applied to collect volatiles from the encapsulated flavours were quite different. The obtained results indicate that there is some effect of fibre polarity on the extraction of terpenic compounds from EO headspace. However, to obtain a more comprehensive explanation of the differences in area response of individual constituents in our study, more detailed investigations with pure compounds (model systems) should be performed and FID response factors

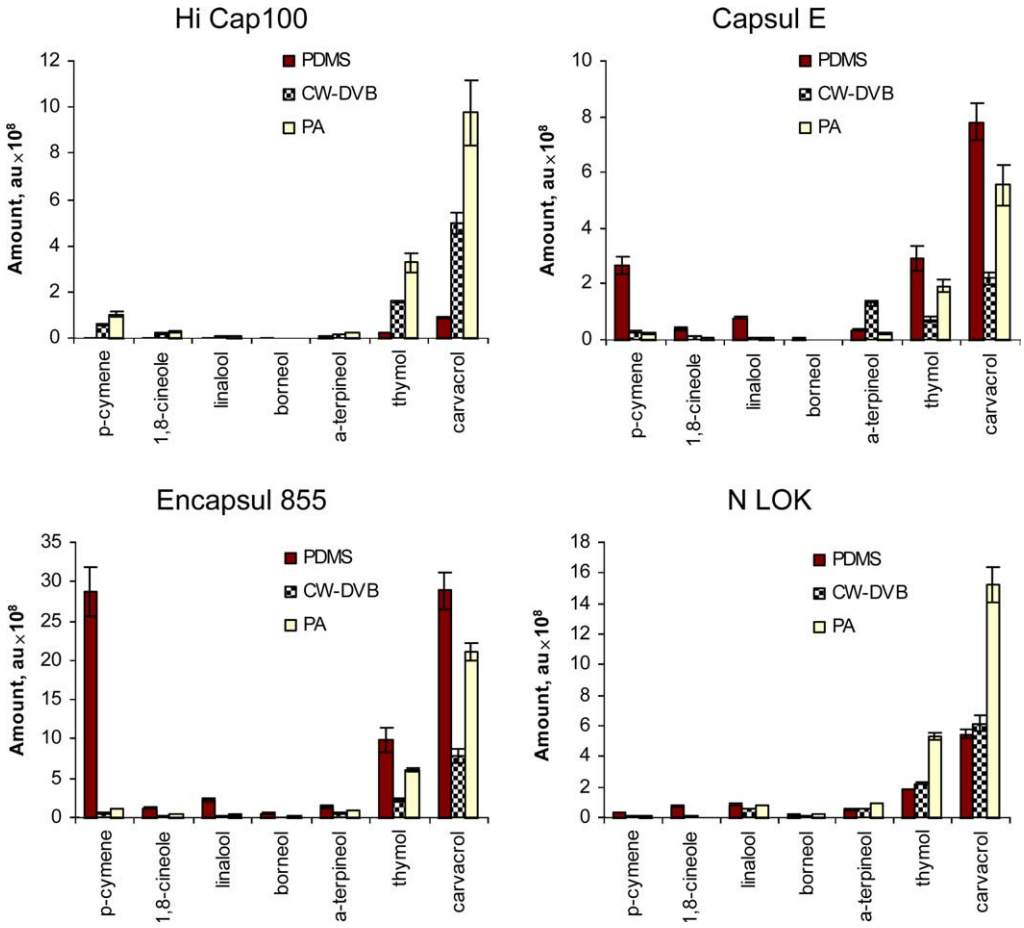

Fig. 3. Flavour profile of the main constituents in the headspace of encapsulated oregano EO, using four different encapsulating matrixes, namely Hi Cap 100, Capsul E, Encapsul 855, N LOK. Determination of the amounts of constituents was performed using SPME–GC–MS, with three different SPME fibers, namely PDMS, CW-DVB and PA.

should be determined. However, the results were repeatable for all encapsulated oils. The precision of SPME measurements was estimated by running three replicate extractions. The corresponding RSD of GC peak area was calculated for all these extractions with each fibre applied. For PDMS extraction the RSD varied from 0.5% (benzaldehyde released from encapsulated into Hi Cap 100 cassia EO) to 19.1% (β-caryophyllene from encapsulated into N LOK thyme oil) and for most of the compounds it was <8%; for CW-DVB it was from 0.9% (benzaldehyde in headspace of cassia essential oil encapsulated into Capsul E) to 19.8% (thymol in headspace of thyme essential oil encapsulated into N LOK), being for most of the volatiles below 10%; for the PA fibre it was from 0.4% (α-terpinene released from encapsulated into N LOK oregano essential oil) to 20.12% (β-caryophyllene in headspace of thyme flavour encapsulated into Encapsul 855 matrix) and for most of the aroma components was less than 11%. Error bars are provided in Figs. 2–4 for every SPME analysis.

Different amounts of volatiles were determined by static headspace above pure oils. Flavour profile above thyme and oregano oils was similar, with major compounds, α-pinene (3.4×10^6 au; 3.2×10^6 au), *p*-cymene (5.0×10^6 au; 3.5×10^6 au) and 1,8-cineole (0.9×10^6 au; 2.2×10^6 au). Monoterpenes are more volatile components than oxygenated hydrocarbons, and, consequently, the phenols, thymol and carvacrol, were detected in remarkably lower amounts, (1.2×10^6 au; 0.2×10^6 au) and (0.1×10^6 au; 0.4×10^6 au), respectively. The major components in headspace of cassia EO were benzaldehyde and (*E*)-cinnamaldehyde, which constituted 0.1×10^6 and 0.5×10^6 au, respectively. Static headspace method was not effective for measuring microencapsulated flavours, due to a very low concentration of volatiles. SPME was more sensitive and effective to measure the release of volatile compounds from thyme, oregano and cassia flavours encapsulated into different coating matrixes at the identical conditions.

3.3. Transient response of gas sensors

After an injection of an odour from the encapsulated oils, pairs of time constant τ_i and corresponding weight

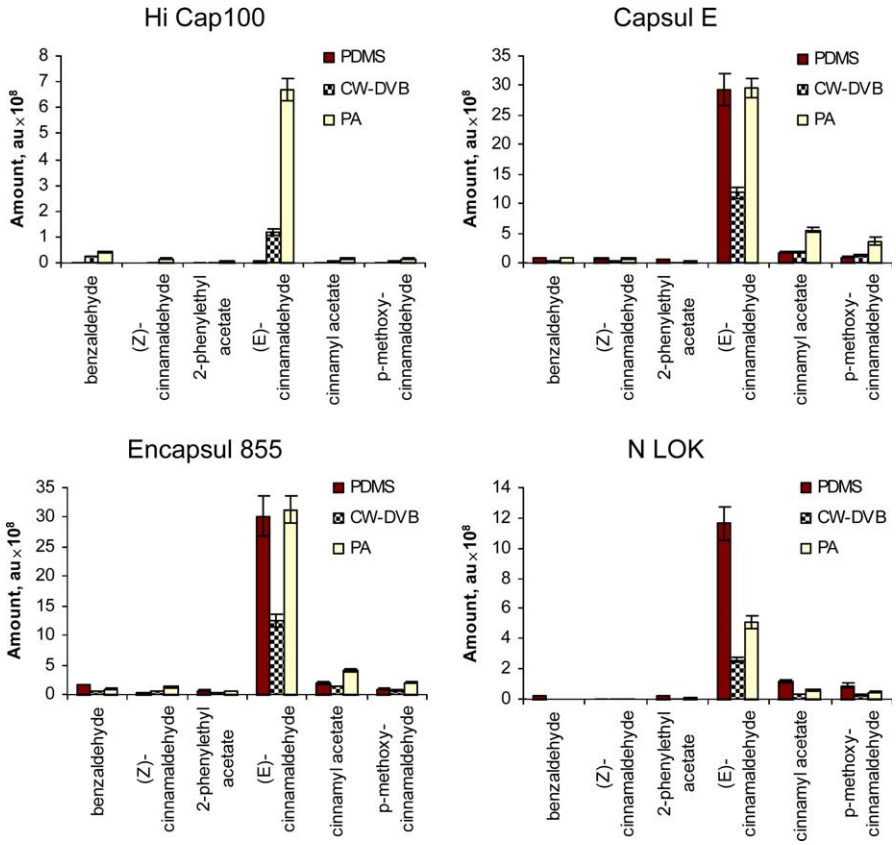

Fig. 4. Flavour profile of the main constituents in the headspace of encapsulated cassia EO, using four different encapsulating matrixes, namely Hi Cap 100, Capsul E, Encapsul 855, N LOK. Determination of the amounts of constituents was performed using SPME–GC–MS, with three different SPME fibers, namely PDMS, CW-DVB and PA.

coefficient a_i were collected for all the sensors in the array. Depending on the coating material and microencapsulated EO, they were extracted from two to four pairs of the parameters. As it was described in (Galdikas et al., 2003), each pair (τ_i, a_i) defined a point in an individual chart composed for a target smell. In Fig. 5, several 2Dτ-images are illustrated for the tested matrixes. Individual image in Fig. 5 corresponds to a certain coating matrix (see labels Hi Cap 100, Capsul E, N LOK, Encapsul 855 on the images). In each image in Fig. 5, the results are summarised for the encapsulated thyme, cassia and oregano flavours detected in our experiments. Reciprocal time scale was used to plot τ_i in the 2Dτ-images because short and intermediate time constants were the target in most cases. Consequently, the long τ-components were concentrated near the zero in these images and are purely distinguished in Fig. 5. A vertical distance from the zero-line upward or downward in the chart illustrates the weight coefficients corresponding with the time constants.

From the Hi Cap 100 image in Fig. 5, it is seen that the (τ_i, a_i)-points were spread for the coating material Hi Cap 100 within some small area around the zero-line. The outlines of this area seemed like an arrow directed along the $1/\tau$-axis (Fig. 5, image Hi Cap 100). This area

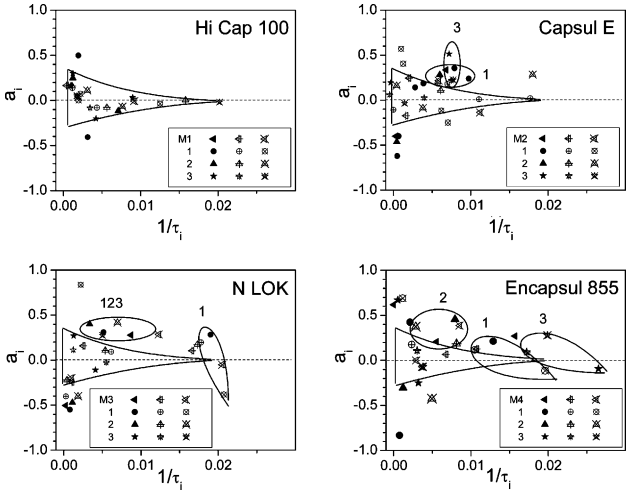

Fig. 5. The 2Dτ-images composed of the time constants τ_i and weight coefficients a_i from transient responses of three gas sensors (SO18-23, SO18-24 and TGS800) to odour released from the EO: thyme – 1, cassia – 2 and oregano – 3, encapsulated in the matrixes: Hi Cap 100 (label M1), Capsul E (label M2), N LOK (label M3) and Encapsul 855 (label M4).

was also drawn in other images in Fig. 5. For other coating materials, only part of the (τ_i, a_i)-points were inside of this small area in the 2Dτ-images. The outside points

were also clustered in some specific areas. These clusters were individual with respect to the flavours in different coatings. In case of Capsul E, the outside clusters were obtained from the transient responses to thyme and oregano. These two clusters (1 and 3) nearly covered each other on the image (Fig. 5, image Capsul E). Two outside clusters were also found in the 2Dτ-image of the N LOK. The cluster 1 in this image was corresponding to the short time constants obtained from the response to thyme encapsulated in the N LOK. The weight coefficients of the short components were big enough to make this cluster distinctive in the chart. The intermediate time cluster marked by 123 in the N LOK image in Fig. 5 consists of the points corresponding to all the flavours tested in our work. According to the 2Dτ-images, the coating material called Encapsul 855 was found to be the most leaking matrix in our study. In the 2Dτ-image of Encapsul 855 in Fig. 5, three clusters were located outside the cluster representing the Hi Cap 100 coating. Each of these outside clusters was individually related with particular oil encapsulated in the Encapsul 855. The shortest τ-constants were extracted from the transient response to oregano in Encapsul 855 (label 3 in the image of Encapsul 855 in Fig. 5). In case of thyme, the τ-constants were longer (cluster labeled by 1) than these for oregano. In the 2Dτ-image of Encapsul 855 in Fig. 5, the cluster 2 corresponding the (τ_i, a_i)-points for cassia was located in the interval of the intermediate time constants. The magnitudes of these constants were the longest ones if compared to the constants in clusters 1 and 3. Some weight coefficients in the cluster 2 were exceeding the reference area twice or even more in the a_i-scale. It means that the intensities of the corresponding components are extremely high.

From some transient responses, very long τ-constants were extracted for the matrixes N LOK, Encapsul 855 and Capsul E. These long τ-constants are illustrated in the charts with normal scaling for the τ_i-axis in Fig. 6. The (τ_i, a_i)-points obtained for the same sensor were scattered near the zero-lines in these charts. Unfortunately, there was not evident relationship between the quality of the coating material and these long constants in the present study. Only the long τ-components labeled by 1 were presented in the approximation of all three matrixes used. Therefore these pairs of the parameters are not discussed thoroughly.

3.4. Comparison of the matrixes

Based on comparison of the 2Dτ-images in Fig. 5, the Hi Cap 100 was supposed to be the least emitting coating material in our study. For the leaking matrixes, individual outside clusters in Fig. 5 were related to the particular flavour released from the coating matrix. In case of Capsul E, thyme and oregano were producing the outside clusters in the 2Dτ-image (labels 1 and 3 in the image Capsul E in Fig. 5). This assumption was supported by the fact, that the outside clusters of the time constants were traced in different places of the 2Dτ-images in Fig. 5 if the responses to similar flavours in different coatings were compared. Since the time constants were equivalent to some effective time for an interaction between the surfaces and individual gas, the outside clusters have to be found in similar positions in 2Dτ-images in Fig. 5 if the sensors detect the same compounds emitted from different coating materials.

The results of the SPME–GC (Figs. 2–4) were analysed along with the 2Dτ-images (Fig. 5) with the aim to attribute the outside clusters to the individual compounds of the flavour. Based on this analysis, the outside clusters of thyme and oregano (labels 1 and 3 in the images Encapsul 855 and N LOK in Fig. 5) were, probably, induced by the response of the sensors to leakage of *p*-cymene and thymol and/or carvacrol, respectively. The smallest detectable concentration of the nonpolar component *p*-cymene on PDMS-coated fibre [$(265.6 \pm 32.19) \times 10^6$] au was in the headspace of oregano EO encapsulated in Capsul E (Fig. 3). If polar coatings were used for the extraction, the smallest concentration of *p*-cymene was obtained in the headspace of thyme EO encapsulated in N LOK and constituted approximately $(10 \pm 1.4) \times 10^6$ au (Fig. 2).

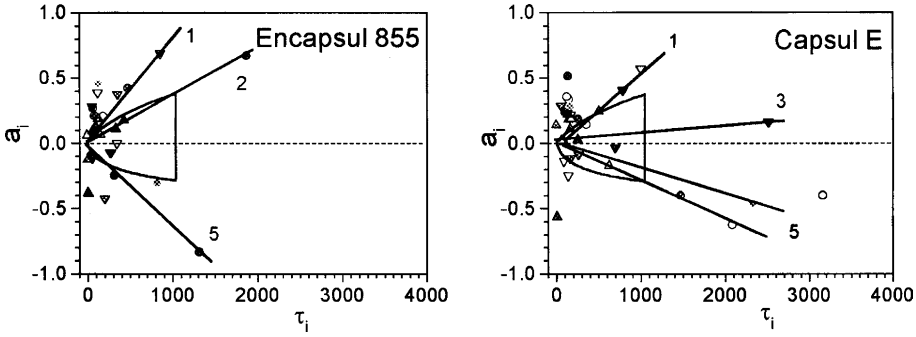

Fig. 6. The 2D-τ-charts (long time constant view) based on the transient responses of the sensors to the odours of the oils encapsulated in the Encapsul 855 and Capsul E matrixes.

The smallest amount of thymol was detected in the headspace of thyme EO encapsulated into Capsul E and this concentration was independent on the fibre used for SPME (Fig. 2). Therefore, it can be supposed that the sensor response was generated by thyme EO above the Capsul E and N LOK matrixes. Assuming the smallest detectable concentration for carvacrol on polar PA-coated fibre equal to $(553.9 \pm 72.7) \times 10^6$ au (oregano EO into Capsul E, Fig. 3), it seems reasonable to suppose that the outside cluster 3 to the right from the "Hi Cap 100 triangle" in the image N LOK in Fig. 5 is not related to carvacrol. The outside clusters of the time constants for cassia might be associated with (*E*)-cinnamaldehyde. The smallest detectable amounts of this component were obtained in the headspace above Encapsul 855 and were equal to $(3023.2 \pm 334.4) \times 10^6$, $(1241.6 \pm 103.2) \times 10^6$ and $(3131.1 \pm 233.9) \times 10^6$ au on PDMS, CW-DVB and PA fibres, respectively (Fig. 4). Since (*E*)-cinnamaldehyde was not detected above other matrixes it is understandable why cassia was detected only if Encapsul 855 was used for microencapsulation. On the other hand, it can be supposed that some volatile compounds undetected by the sensors are also emitted from the coating. For example, the amount of benzaldehyde extracted with PDMS in the headspace above Encapsul 855 was $(163.8 \pm 7.8) \times 10^6$ au, while the amount of this compound above Capsul matrix was 2.4 times lower [$(68.3 \pm 2.1) \times 10^6$ au] (Fig. 4).

We should take into account that the parameters of the transient response are probably influenced by coadsorption of several volatile compounds. In most cases, the effect of the coadsorption leads to a summation of the partial signals. Only the amount of the dominant compound might be evaluated by the e-nose. For this reason, sensor arrays have to be calibrated with respect to the pure compounds before the quantitative evaluation can be performed by the e-nose. On the other hand, the calibration is not essential if only qualitative and rapid (on-line) grading of the coating materials is required for a practical application.

It must be added, that the reproducibility of the response signals depends on (1) the stability of the sensors and (2) the stability of the smell source. It was demonstrated in our recent study (Galdikas et al., 2003) that the reproducibility of the sensor responses is high (standard deviation for the extracted parameters is about ±10–15%) if the array is exposed to the well-controlled composition of the synthetic atmosphere. The differences between the parameters exposed by the e-nose were mainly originated by the changes in the smell-source. Since the e-nose method is extremely sensitive to any changes of the smell composition, the differences between the images delayed by several hours were significant. It seems reasonable to suppose that the concentration of the lightweight compounds might decrease during long tests.

4. Conclusion

Phenomenological parameters that describe the kinetics of the response of metal oxide sensors to a steep change in gas composition were used as the variables for the description of the features of the target smell. It was demonstrated that the rise of the response contains information about the features of the smell emitted from the microencapsulated flavours.

The reproduction of the 2Dτ-images was satisfactory in the tests repeated during some fixed period under unchanged conditions. The parameters of the sensor response were located within the areas associated with specific flavour. It should be noted, that the identification of individual volatile components of the smell was difficult due to limitation of the features described by the method of the signal analysis. In spite of this, it is clear that the method is highly effective for the comparative analysis of the smell features while the absolute recognition of the components requires thorough analysis and calibration with respect to the pure volatile components of the smell.

Even after the calibration the e-nose method can not be used as an analytical method instead of the standard ones (e.g. GC–MS). On the other hand, our study suggests that the e-nose method is acceptable for a rapid (on-line) evaluation/comparison of the coatings in a practical application. We recognise that an increase of the response rate is desirable for this. High sensitivity of the e-nose to small changes in the smell-source offers an opportunity to evaluate the leakage of the flavour from the matrixes, however, a calibration of the e-nose is difficult using the non-stable target sample. We think that some special calibration routine has to be developed for such type of the test-samples before the reliability of the recognition of the leakage level or the matrix with the flavour can be correctly characterised.

Acknowledgement

Partial financial support from the Lithuanian State Foundation of Science and Studies (Project No: V-03042, COST 921) is gratefully acknowledged.

References

Adams, R. P. (2001). *Identification of essential oils components by gas chromatography/quadrupole mass spectroscopy* (p. 456). Illinois, USA: Allured Publishing Corporation.

Ampuero, S., & Bosset, J. O. (2003). The electronic nose applied to dairy products: A review. *Sensors and Actuators B, 94*, 1–12.

Baranauskienė, R., Venskutonis, P. R., Dewettinck, K., Verhé, R. (2003). Microencapsulation properties of thyme (*Thymus vulgaris*

L.) essential oil. In *NFIF, New Functional Ingredients and Foods*, April 9–11, Copenhagen: Denmark.

Baratta, M. T., Dorman, H. J. D., Deans, S. G., Figueiredo, A. C., Barroso, J. G., & Ruberto, G. (1998). Antimicrobial and antioxidant properties of some commercial essential oils. *Flavour and Fragrance Journal, 13*, 235–244.

Brezmes, J., Llobet, E., Vilanova, X., Orts, J., Saiz, G., & Correig, X. (2001). Correlation between electronic nose signals and fruit indicators on shelf-life measurements with pinklady apples. *Sensors and Actuators B, 80*, 41–50.

Bylaitė, E., Venskutonis, P. R., & Maždžierienė, R. (2001). Properties of caraway (*Carum carvi* L.) essential oil encapsulated into milk protein-based matrices. *European Food Research and Technology, 212*, 661–670.

Di Natale, C., Olafsdottir, G., Einarsson, S., Martinelli, E., Paolesse, R., & D'Amico, A. (2001). Comparison and integration of different electronic noses for freshness evaluation of cod-fish fillets. *Sensors and Actuators B, 77*, 572–578.

Galdikas, A., Kancleris, Ž., Senulienė, D., & Šetkus, A. (2003). Influence of heterogeneous reaction rate on response kinetics of metal oxide sensors to gas: Application to the recognition of an odour. *Sensors and Actuators B, 95*, 244–251.

Galdikas, A., Mironas, A., Senulienė, D., & Šetkus, A. (2000). Specific set of the time constants for characterisation of organic volatile compounds in the output of metal oxide sensors. *Sensors and Actuators B, 68*, 335–343.

Guadarrama, A., Fernandez, J. A., Iniguez, M., Souto, J., & de Saja, J. A. (2001). Discrimination of wine aroma using an array of conducting polymer sensors in conjunction with solid-phase microextraction (SPME) technique. *Sensors and Actuators B, 77*, 401–408.

Hulin, V., Mathot, A. G., Mafart, P., & Duffose, L. (1998). Antimicrobial properties of essential oils and flavor compounds. *Sciences Des Aliments, 18*, 563–582.

Katoa, K., Katoa, Y., Takamatsua, K., Udakaa, T., Nakaharaa, T., Matsuuraa, Y., et al. (2000). Toward the realization of an intelligent gas sensing system utilizing a non-linear dynamic response. *Sensors and Actuators B, 71*, 192–196.

Lide, D.R. (2004). *CRC handbook of chemistry and physics 2003–2004* (84th ed., p. 2616). LLC, New York: CRC Press.

Maekawa, T., Suzuki, K., Takada, T., Kobayashi, T., & Egashira, M. (2001). Odor identification using a SnO_2-based sensor array. *Sensors and Actuators B, 80*, 51–58.

Marino, M., Bersani, C., & Comi, G. (1999). Antimicrobial activity of the essential oils in *Thymus vulgaris* L. using a bioimpedometric method. *Journal of Food Protection, 62*, 1017–1023.

Nakata, S., Takemura, K., & Neya, K. (2001). Non-linear dynamic responses of a semiconductor gas sensor evaluation of kinetic parameters and competition effect on the sensor response. *Sensors and Actuators B, 76*, 436–442.

Nielsen, P. V., & Rios, R. (2000). Inhibition of fungal growth on bread by volatile components from spices and herbs, and the possible application in active packaging, with special emphasis on mustard essential oil. *International Journal of Food Microbiology, 60*, 219–229.

Penza, M., Cassano, G., Tortorella, F., & Zaccaria, G. (2001). Classification of food, beverages and perfumes by WO_3 thin-film sensors array and pattern recognition techniques. *Sensors and Actuators B, 73*, 76–87.

Rasooli, I., & Abyaneh, M. R. (2004). Inhibitory effects of Thyme oils growth and aflatoxin production by *Aspergillus parasiticus*. *Food Control, 15*, 479–483.

Shirey, R. E. (1999). SPME fibers and selection for specific applications. In S. A. Scheppers Wercinski (Ed.), *Solid phase microextraction. A practical guide* (pp. 59–110). New York, NY, USA: Marcel Dekker.

Shirey, R. E. (2000a). Optimization of extraction conditions and fibre selection for semivolatile analytes using solid-phase microextraction. *Journal of Chromatographic Science, 38*, 279–288.

Shirey, R. E. (2000b). Optimization of extraction for low-molecular-weight analytes using solid-phase microextraction. *Journal of Chromatographic Science, 38*, 109–116.

Simona, I., Barsan, N., Bauera, M., & Weimar, U. (2001). Micromachined metal oxide gas sensors: Opportunities to improve sensor performance. *Sensors and Actuators B, 73*, 1–26.

Steffen, A., & Pawliszyn, J. (1996). Analysis of flavor volatiles using headspace solid-phase microextraction. *Journal of Agricultural and Food Chemistry, 44*, 2187–2193.

Ultee, A., & Smid, E. J. (2001). Influence of carvacrol on growth and toxin production by *Bacillus cereus*. *International Journal of Food Microbiology, 64*, 373–378.

Velluti, A., Sanchis, V., Ramos, A. J., Egido, J., & Marín, S. (2003). Inhibitory effect of cinnamon, clove, lemongrass, oregano and palmrose essential oils on growth and fumonisin B_1 production by *Fusarium proliferatum* in maize grain. *International Journal of Food Microbiology, 89*, 145–154.

Venskutonis, P. R., Boceviciute, R., Plaušinaitis, R. (2001). Instrumental and sensory evaluation of microencapsulated essential oils. In M. Rothe (Ed.), *Flavour 2000 perception, release, evaluation, formation, acceptance, nutrition/health: Proceedings of the 6th wartburg aroma symposium*, Eisenach, 10–13 April 2000 (pp. 67–85). Eigenverlag Bergholz-Rehbrücke.